Supplemental Data

Document S1. Supplemental Experimental Procedures, Eight Figures, and One Table. (see next page)

Movies S1A & S1B

1A is a confocal timelapse movie of embryonic macrophages that express a UAS::GCaMP1.6 transgene under the control of crq::Gal4 (green) overlayed with DIC, showing the dynamic changes in intracellular Ca2+ levels as visualized by this reporter. High levels of GFP expression reflects high levels of intracellular Ca2+ and low GFP expression reflects low intracellular Ca2+ concentration. 1B is the corresponding timelapse movie showing the GFP channel only, where fluctuations in GFP expression levels can be fully appreciated. Both movies are played at 5 frames/s. Images were taken every 60 s for 60 min.

Movie S2

This movie shows a magnified view of GCaMP1.6-expressing macrophages (in green), one of which (green arrow) shows high levels of GFP expression prior to engulfing an apoptotic corpse (red arrow pointing to DIC bright round corpse during the movie). This engulfment event is quickly followed by a decrease in GFP fluorescence. This is not due to bleaching of the sample as remaining GFP fluorescence can be observed on the second macrophage nearby and is consistent with a previous study reporting similar results during engulfment events by mammalian phagocytes (Dewitt and Hallett, 2002).

Movie S3

This movie shows a magnified view of GCaMP1.6-expressing macrophages (in green), one of which (green arrow) quickly migrates towards the site of bacteria (red arrow). After coming into close contact with a first single bacterium, the color of which changes from red to a slightly discolored red/orange, the macrophage then ignores this bacterium and continues to migrate towards two bacteria without showing any changes in its GCaMP fluorescence. The single bacterium it bypassed returns to a bright red color. When the macrophage reaches the two bacteria, they too change from a bright red to a slightly discolored red/orange appearance. In contrast with the first bacterium, this discoloration persists in these two bacteria and is followed by a drop in GCaMP fluorescence in the macrophage, thereby suggesting that the bacteria have been fully ingested in a mature acidified phagosome. Of note, however, is that this experiment does not allow us to fully exclude the possibility that the bacteria were not yet fully ingested when this drop in GCaMP fluorescence occurred.

Cell, Volume *135*

Supplemental Data

Undertaker, a *Drosophila* Junctophilin, Links Draper-Mediated Phagocytosis and Calcium Homeostasis

Leigh Cuttell, Andrew Vaughan, Elizabeth Silva, Claire J. Escaron, Mark Lavine, Emeline Van Goethem, Jean-Pierre Eid, Magali Quirin, and Nathalie C. Franc

Supplemental Text

Characterization of an apoptotic cell-phagocytosis assay in S2 cells.

At 26ºC, the number of S2 cells engulfing apoptotic cells increased over time with about 60% of S2 cells showing some phagocytic activity after 24 hours (**supplementary figure 2C**). As expected, phagocytosis of apoptotic cells by S2 cells was completely inhibited by cytochalasin D, a drug that blocks actin polymerization (**data not shown**). To ensure that the fixation and labelling of apoptotic cells did not interfere with their recognition and engulfment, we also carried out competition experiments in which S2 cells were incubated for 5 hours with FITC-labelled fixed apoptotic cells and either an equal number, or 10 fold-excess of freshly prepared unlabelled non-fixed apoptotic cells. These could compete with fixed FITC-labelled apoptotic cells, with a 50% competition rate observed at a 1:1 ratio, confirming that fixation and labelling of apoptotic cells did not mask their “eat me” signals, nor affect the ability of S2 cells to engulf them (**supplementary figure 2D**).

Supplemental Experimental Procedures:

Single embryo polymerase chain reactions (sePCRs):

Mapping of the deletions by sePCRs were performed as previously described in (Franc et al., 1999). Primers used were as follows: cno_S: 5' GCCATTTGGCTGACCCAGCATTCC 3', cno_AS: 5' CCGAATCACAGCCTTAGTCTTAGC 3' (396 bp on genomic, 269 bp on cDNA); CG31537_S: 5' CCTTCTTCATTCAGTGGCTGATG 3', CG31537_AS: 5' CCTCCTCACCGCCGGTGAGACG 3' (347 bp on genomic, 347 bp on cDNA); CG12161_S: CTGCAGCTCAATAATTTTGCGGC 3', CG12161_AS: 5' CCACGCATTATGTTCAACGGC 3' (779 bp on genomic, 384 bp on cDNA); CG1116_S: 5'CCGACGAACTTCCCGTAACCG 3', CG1116_AS: 5' CCGAGCTTATACGCTGGCTTG 3' (272 bp on genomic, 206 bp on cDNA); CG1115_S: 5' GGGTCCCCTGATGCCCATGCC 3', CG1115_AS: 5' AGGCAGAGATGTGTGTACCAG 3' (551 bp on genomic, 342 bp on cDNA); Katanin 60_S: 5' CCGGCATGAGCATTGGCAGCACG 3', Katanin 60_AS: 5' GGACGACGACTCCACCGCTGC 3' (444 bp on genomic, 250 bp on cDNA); Mms19_S: 5' GCTCTACCGCGGGCCCAGATTCC 3', Mms19_AS: 5' GGCCAAATGCAGCAGCGGATACG 3' (480 bp on genomic, 268 bp on cDNA); CG10233_S: 5' GAAAGAATCCCTCGTTTCTGGG 3', CG10233_AS: 5' ACATCGGCGAGTGGAACCAGCG 3' (512 bp on genomic, 331 bp on cDNA); CG12163_S: 5' TCGGCCCACTCCACGGATCGCG 3', CG12163_AS: 5' CGCAGCAGACGCAGCGCGAACG 3' (632 bp on genomic, 338 bp on cDNA); CG1113_S: 5' CGTGCAATAACTGTCCGGCTCCG 3', CG1113_AS: 5'

AGTTGGAGCAGTTGCTGCCTGAG 3’ (480 bp on genomic, 275 bp on cDNA); CG12173_S: 5’ AGTACGGCTGCAGGTTCCCGGCC 3’, CG12173_AS: 5’ GCGGACTACAAGGCCCTGTTAAG 3’ (613 bp on genomic, 304 bp on cDNA); Tim17a2_S: 5’ GGGGCGGAGTTAGAGCGGGT 3’, Tim17a2_AS: 5’ GCCAACTGCTCCACCGCCCAG 3’ (750bp on genomic, 398bp on cDNA); l(3)82Fd_S: 5’ TGGCCTGTGGCTGGATGGTGATCTGAAC 3’, l(3)82Fd_AS: 5’ AAATAGATAGGTCGGCAGGAGGCCCTC 3’ (197 bp on genomic and cDNA); Tim17b1_s: 5’ TCGAAACGCCCCCTCCGGCCTGG 3’, Tim17b1_AS: 5’ TAGGAATCCGCCGAATAATGGG 3’ (503 bp on genomic, 312 bp on cDNA); CG11999_S: 5’ CGCTGGTAGGCAGCATTTCCAGG 3’, CG11999_AS: 5’ CGCACGGTGGATCCGCAGGCG 3’ (383 bp on genomic, 256bp on cDNA); CG1161_S: 5’ GAGACTGCGGCGCAGACATTCCC 3’, CG1161_AS: 5’ GGTGTGCTCCTGGTAGTTCGCC 3’ (790 bp on genomic, 447 bp on cDNA); CG12000_S: 5’ CTACAACAGCCTAGCGCAGCCC 3’, CG12000_AS: 5’ CGCCGAGCAGGATGTTCTTGTTG 3’ (360 bp on genomic, 293 bp on cDNA); CG16708_S: 5’ GGCAGCCCAGAGCGAGAACTACC 3’; CG16708_AS: 5’ TCGCGCCGCAGATCATAAAGAAA 3’ (475 bp on genomic and cDNA); CG16708P_S: 5’ CAGGATGGAACGTTTATCCATAC 3’, CG16708P_AS: 5’ CAGTTATATGTACGGTCACACTG 3’ (369 bp on genomic and cDNA); CG31542_S: 5’ GTCTCCGTGTGGCAAGTGCAAC 3’, CG31542_AS 5’ CTGTCATGTCATGTTGTGAGCG 3’ (687 bp on genomic, 666 bp on cDNA); Rpll18_S: 5’ CAGTGATGGATGATGCGGACTAC 3’, Rpll18_AS: 5’ TCAGCTCTTTCATGGCGATCTGC 3’ (367 bp on genomic, 309 bp on cDNA);

CG2669_S: 5’ TCACCAGCTTCGTGCGCTGCATG 3’, CG2669_AS: 5’ ACTGTGCTGATGGCACTCTTGGC 3’ (714 bp on genomic and cDNA); CG14667_S: 5’ GAGATTGTTTGCGAGCGCTGC 3’, CG14667_AS: 5’ TGCGCAAGCTGACAAGCTTAC 3’ (819 bp on genomic); 7B2_S: 5’ TCGCCTTGAGTGGCTAACAGGTC 3’, 7B2_AS: 5’ ACGTCGTGTATGCTCGCGTTATC 3’ (800 bp on genomic and cDNA); CG14668_S: 5’ CGTGTAGCCAGCAATGCAATAAG 3’, CG14668_AS: 5’ AGAACTCGGCGACACTTGAGCAG 3’ (818 bp on genomic and cDNA); Kkv_S: 5’ AGAGCTGCGCGGACGGCAGCG 3’, Kkv_AS: 5’ TTGGCACTGACTCTCCTCTGC 3’ (807 bp on genomic); Kkv_S: 5’ TATCCATTTAGAGCGCCCAC 3’, Kkv_AS: 5’ AGAACTCATTGAATCCCTCG 3’ (822 bp on genomic); CG1172_S: 5’ TGCCAGCGATGGTTCTACAGC 3’, CG1172_AS: 5’ CTGCACTGCCTAAATCAGTTG 3’ (638 bp on genomic and cDNA); Or83a_S: 5’ GACGACTCCAAGCGTCGCGACC 3’, Or83a_AS: 5’ CACCATATGCAGGCCACTGGAG 3’ (691 bp on genomic, 623bp on cDNA); CG2663_S: 5’ TCTTGAGCGCTTCGGTTGTGTCG 3’, CG2663_AS: 5’ CCGCAACTGTATGTGCACTCATG 3’ (596 bp on genomic, 465 bp on cDNA); Or83b_S: 5’ GCAGCTGCTCGCAGGCGAATATC 3’, Or83b_AS: 5’ ATGACAACCTCGATGCTGCCGAG 3’ (763 bp on genomic, 694 bp on cDNA); CG12147_S: 5’ GCCTGCGTAGAAGTCTGGCAAGC 3’, CG12147_AS: 5’ CAGTCCGAAGTCAATCATGTAC 3’ (666 bp on genomic and cDNA); CG14669_S: 5’ GGGAATCCGCCAGAAGC 3’, CG14669_AS: 5’ GCGCCGCCTCCTCCTAC 3’ (911 bp on genomic). In all reactions, a RP49 primer set was used as an internal control

for the presence of DNA. RP49_S: 5' ATACAGGCCCAAGATCGTGA 3', RP49_AS: 5' GTGTATTCCGACCACGTTACA 3'. PCR cycles were as follows: 94˚C for 5 min for one cycle, denaturation at 94˚C for 1 min, annealing at 65˚C for 1 min, extension at 72˚C for 1 min 15 sec, for 30 cycles, and final extension at 72˚C for 10 min. 15 µl of each PCR reaction were loaded onto a 2% agarose/TBE (Tris/Borate/EDTA) gel and their products were separated, visualized and photographed on a Syngene genelink trans-illuminating system.

RNA interference:

For the amplifications of amplicons that were span introns, total mRNA of wild-type embryos was extracted using Qiagen RNeasy mini kit and Qiashredder columns following manufacturer's protocol, including RNAse-free DNAse digestion steps. RNA was eluted in 30 µl of RNAse-free dH_2O. First-strand cDNA synthesis was performed with 8 µl of RNA extract using the superscript^{TM} first-strand synthesis for RT-PCR kit from Invitrogen. 2 µl of cDNA preparations were used in PCRs using 2 µl of primer mix at 10 µM each and 48 µl of Platinum pfx DNA polymerase supermix (Invitrogen), using the same PCR conditions as described in Material and Methods section of this manuscript. PCR amplicons for *rab5*, *uta*, *dstim*, *dorai*, *drpr*, *drced-6*, *crq and pall* RNAi experiments were amplified using primer sequences corresponding to DRSC31655, DRSC12132, DRSC20158, DRSC22061, DRSC38541, DRSC38500, DRSC00810, DRSC36242 amplicons, respectively, which can be found on the DRSC public web site at http://flyrnai.org// These are predicted to have no off-targets (using 19bp sequence comparison). Primers for *eater* RNAi were: Eater T7 Forward, 5'-TTA ATA CGA CTC

ACT ATA GGG AGA AAC GTT CAA ACG AGG GAT TG-3', Eater T7 Reverse, 5'-TTA ATA CGA CTC ACT ATA GGG AGA GGT GGT TGG ATT CAG CTT GT-3'.

Plasmid construct:

The EST *GH04877* encodes *CG10233* (Berkeley Drosophila Genome Project (BDGP)). Its cDNA insert was excised from the *pOT2* vector by *XhoI/BglII* restriction digests using 5 Units of enzymes and appropriate buffer in the presence of 0.1 mg/ml of BSA. Both cDNA insert and *XhoI/BglII* digested *pUAST* vector were ligated using 5 Units of T4 DNA ligase in a 20 μl final volume overnight at room temperature. 1 μl of ligation was electroporated into *DH5α* bacteria from Invitrogen using a Bio-Rad electroporator and following manufacturer's instructions. Transformed bacteria were grown in 1 ml of SOC medium (Gibco) in a bacterial shaker at 37ºC, and subsequently plated onto LB agar plates containing 100 μg/ml of ampicillin and incubated overnight at 37ºC. Single colonies were picked and grown into 2 ml of LB medium containing 50 μg/ml of ampicillin. Preparations of plasmid DNA were performed using the Qiagen mini-prep kit. Individual clones containing the insert were identified by restriction map analysis and gel electrophoresis. Restriction digests were all conducted for one hour at 37ºC and made use of 5 μl of each plasmid preparations and 5 Units of appropriate restriction enzymes in 20 μl final volume containing 10 % of appropriate buffer and 0.1 mg/ml of BSA.

Latex beads/pHrodo bacteria competition:

An aqueous solution of 0.9 μm latex beads was diluted one in two in PBS. 138nL of the diluted suspension was injected into the thoraces of adult males using a Drummond

Scientific Nanoject II. Animals were allowed to recover for one hour at 25ºC before proceeding with pHrodo-labeled bacterial injection as described in the Material and Methods of this manuscript.

Bacteria injection in embryos:

TRITC-labelled E. coli bioparticles (Molecular probes) injections were performed as previously described in (Franc et al., 1999).

Quantitative PCR:

1-2x10^6 RNAi-treated cells were pelleted and frozen in liquid nitrogen, and sent to SeqWright for relative qPCR analysis according to their standard Taqman protocol. Primer/probe sequences for detection of *RpL32, rab5, uta, stim, orai, drCed-6,* and *drpr* were as follows:

RpL32 forward primer 5'-GCGCACCAAGCACTTCATC-3', reverse primer 5'-CATTTGTGCGACAGCTTAGCA-3'; probe 5'-6FAM-CCACCAGTCGGATCG-3';

rab5 forward primer 5'-CCTGGGTCAAGGAACTGCAT-3', reverse primer 5'-GGCCAGCGCAATGACAA-3', probe 5'-6FAM-AACAAGCCTCACCAAAC-3';

uta forward primer 5'-GGACGACTACGATGATGACATGA-3', reverse primer 5'-GTTGGTGCTGGTTCTCGATTC-3', probe 5'-6FAM-CGTGGGCGTGACCA-3';

stim forward primer 5'-CTGAGCGAGTCCGATGACTTT-3', reverse primer 5'-TTTCGTAGCCCGAGTCGTACTT-3'; probe 5'-6FAM-TGCGGGAGGAATT-3';

orai forward primer 5'-CCTGTCCTGGCGGAAGCT-3', reverse primer 5'-CGTCTTGCTGGATGCCTTTAG-3', probe 5'-6FAM-CAGCTTAGTCGGGCCAA-3';

drced-6 forward primer 5'-GGCAAGCTGGATGATGATAAGC-3', reverse primer 5'-GCTGGGCGACGCTGAGT-3', probe 5'-6FAM-TCGACACCAATTCC-3';
drpr forward primer 5'-GAACGGTGCCCGGAGATC-3', reverse primer 5'-CAGAGAATTTCACCTGTGATGTGAT-3', probe 5'-6FAM TCCATGGCAACAAGAG-3';
crq forward primer 5'-TGGCCGGGTATTGCAGAT-3', reverse primer 5'-CCCGGGCTTGAGGGTAA-3', probe 5'-6FAM-ACCTTGTAGAGGATGGC-3'
eater forward primer 5'-ATAACGATCCATCTAACCGATGTGT-3', reverse primer 5'-GATTGGCAGGTTCCTCGACTAC-3', probe 5'-6FAM-CCCTACTGCAAGGGA-3'.

Supplemental References

Dewitt, S., and Hallett, M.B. (2002). Cytosolic free Ca(2+) changes and calpain activation are required for beta integrin-accelerated phagocytosis by human neutrophils. The Journal of cell biology *159*, 181-189.

Franc, N.C., Heitzler, P., Ezekowitz, R.A., and White, K. (1999). Requirement for croquemort in phagocytosis of apoptotic cells in Drosophila. Science *284*, 1991-1994.

Kocks, C., Cho, J.H., Nehme, N., Ulvila, J., Pearson, A.M., Meister, M., Strom, C., Conto, S.L., Hetru, C., Stuart, L.M., *et al.* (2005). Eater, a transmembrane protein mediating phagocytosis of bacterial pathogens in Drosophila. Cell *123*, 335-346.

Stuart, L.M., Deng, J., Silver, J.M., Takahashi, K., Tseng, A.A., Hennessy, E.J., Ezekowitz, R.A., and Moore, K.J. (2005). Response to Staphylococcus aureus requires CD36-mediated phagocytosis triggered by the COOH-terminal cytoplasmic domain. The Journal of cell biology *170*, 477-485.

Supplemental Figure Legends:

<u>Figure S1</u>: Phagocytosis of apoptotic cell defects in *Df(3R)3-4* deficiency macrophages that are fully differentiated and functional.

A-B are macrophages of stage 13 embryos stained with CRQ Ab to mark macrophages (green) and 7-AAD that brightly stains apoptotic corpses (red). In A, numerous large wild-type macrophages located in the head region of the embryo strongly express CRQ and engulf multiple apoptotic cells. In B, *Df(3R)3-4* homozygous mutant macrophages appear smaller than in wild-type, with most apoptotic cells seen outside but in close proximity to the macrophages. Dotted white circles are indicative of single macrophage cell size. In C and D are high magnification views of macrophages from wild-type and *Df(3R)3-4* homozygous mutant embryos, respectively, which were injected with DIAcLDLs. Endocytic vesicles containing DIAcLDLs seen in red are present in both macrophages that are expressing *UAS::eGFP* under the control of the *crq::Gal4* driver (green). Of note is the presence of large vesicles within wild-type macrophage that are likely to contain engulfed apoptotic cells, while the mutant macrophage lacks such vesicles reflecting its defect in phagocytosis of apoptotic cells and appears smaller in size. Scale bars in A-B are 10 μm and 5μM in C and D.

E-G are lateral views of the head region of a wild-type (E), *Df(3R)ED5156* (F), and *Df(3R)ED5138* (G) homozygous embryos. In H and I are the respective magnified counterparts of E and F. In I, homozygous *Df(3R)ED5156* mutant macrophages engulf multiple apoptotic cells and appear large with strong CRQ expression, as seen in wild-type embryos in H. Scale bars in E-G are 50 μm and 10 μm in H-I.

Figure S2: Characterization of an assay for phagocytosis of apoptotic cells by S2 cells.

In A and B are phagocytosis assays in S2 cells conducted at 26˚C (control A), or at 4˚C (B). Fully engulfed FITC-labelled apoptotic S2 cells appear green. CTB-stained live S2 cells appear blue. While FITC-labelled apoptotic cells can be seen in A, none are detected at 4˚C in B. Graphs presented in C and D are representative of three independent phagocytosis assays for which we manually counted at least 100 cells per assay. Total number of S2 cells having engulfed at least one apoptotic cell was counted and divided by the total number of cells present within the field of view to establish the percentage of engulfing S2 cells. Bars represent the mean percentages ± SD. In C, apoptotic cells were incubated for 1, 3, 5 or 24 hrs to allow for their engulfment. The number of phagocytosing S2 cells increases over time with over 60% of cells having engulfed apoptotic cells by 24 hrs. In D, fixed FITC-labelled apoptotic cells were co-incubated with increasing ratios of unlabelled non-fixed apoptotic cells for 5 hours. Unlabelled non-fixed apoptotic cells competed efficiently at a 1:1 ratio with labelled apoptotic cells. T-Tests returned p values of less than 0.005. In E and F are phagocytosis assays in S2 cells that were mock- (E), or RNAi-treated with dsRNA for *Rab5* (F) prior to incubation with FITC-labelled apoptotic cells. A significant reduction in phagocytosis of apoptotic cells was observed when *Rab5* was down-regulated (F), as compared with mock-treated cells (E). Scale bars in A-B and E-F are 200 μm.

<u>Figure S3</u>: Assessment of phagocytosis assay specificity and sensitivity to Ryanodine and BTP-2 treatments.

In A, B and C are bar graphs relating the percentages ± SEM of engulfing cells after treatment of S2 cells with 200 μM ryanodine, or 1 μM of BTP-2, two drugs that respectively block the ER Ca^{2+} channels known as Ryanodine receptors, and plasma membrane CRAC channel known as Orai, respectively; or after RNAi-treatment of S2 cells to knock-down *crq* and *eater* that were incubated in the presence of apoptotic cells (A), pHrodo *E. coli* (B) or pHrodo *S. aureus* (C). Both drugs inhibited all phagocytic events. Although we currently have no explanation for this, BTP-2 appeared less potent at inhibiting apoptotic cell-engulfment than that of bacteria. While *crq* RNAi-treated cells were less efficient at engulfing apoptotic cells and *S. aureus*, they engulf *E. coli* as efficiently as control mock-treated cells, as previously reported (Stuart et al., 2005). *eater* RNAi-treated cells failed to efficiently engulf both *E. coli* and *S. aureus* but engulfed apoptotic cells similarly to mock-treated S2 cells, as previously reported (Kocks et al., 2005).

<u>Figure S4</u>: Heterogeneity in response to TG in S2 cells.

Graphs of the changes in fluo-3AM fluorescence in mock- or *uta* RNAi-treated S2 cells exposed to 2.5 μM TG in Ca^{2+}-free medium at 30 sec and to 2 mM extracellular Ca^{2+} 150 sec later. Results are given as a fold increase of the mean fluo-3 fluorescence measured over time, each coloured trace corresponding to the results obtained for individual cells. *uta* RNAi-treated failed to trigger the opening of the CRAC channel compared to mock

cells, as they failed to respond to Ca^{2+} addition. Both Mock- and *uta* RNAi-treated S2 cells were heterogeneous in their response to TG.

<u>Figure S5</u>: *uta* RNAi-treated S2 cells respond to Ca^{2+} addition as efficiently as mock-treated S2 cells in absence of thapsigargin treatment.

A summarizes changes over time in fluo-3AM fluorescence in mock- and *uta* RNAi-treated S2 cells that were plated in Ca^{2+}-free medium and exposed to 2 mM extracellular Ca^{2+}. Results are given as a fold increase of the mean fluo-3 fluorescence measured over time of two independent experiments. Mock-treated cells triggered Ca^{2+} entry by a store-independent mechanism that was preserved in *uta* RNAi-treated cells. Of note is that the amplitude of the fluorescence following Ca^{2+} addition reported in this set of experiments cannot be compared to that of figures 4E and 6E, which were carried out on separate days. B is a graph showing changes in fluo-3AM fluorescence in control cells left untreated or treated with 2.5 μM TG followed by 2 mM Ca^{2+}. TG-treated cells have higher levels of intracellular Ca^{2+} than in untreated cells, consistent with the opening of both ER-dependent and ER-independent Ca^{2+} channels in TG-treated cells versus the opening of ER-independent Ca^{2+} channels only in untreated cells.

<u>Figure S6</u>: *dorai* gene structure and mapping of *dorai* P-element insertions mutations.

Schematic representation of the *dorai* gene structure and corresponding predicted five mRNA isoforms, including the loci of both *P{lacW}olf186-Fk11505* and *P{EPgy2}olf186-FEY09167* in proximity to the first and second exons, the precise

mapping of which can be found in their respective flybase reports at http://flybase.bio.indiana.edu/.

Figure S7: Characterization of the pHrodo bacterial engulfment assays.

In A and B, S2 cells were incubated with pHrodo *E. coli* at 26ºC either in absence (control in A) or in presence of 10 μM cytochalasin D (B), which blocks actin polymerisation. In the latter, cells failed to engulf pHrodo *E. coli* demonstrating that, as expected, phagocytosis of pHrodo *E.coli* is actin-dependent. In C and D, S2 cells were incubated with pHrodo *S. aureus* at 26ºC (control in C) or at 4ºC (D), which is non-permissive to particle internalization. In the latter, we failed to observe any pHrodo fluorescence of *S. aureus* demonstrating that, as expected, *S. aureus* may be bound but not internalized by S2 cells, thereby preventing the fluorescence of its pHrodo component, which is dependent on particle internalization into matured phagosomes. Although not shown here, we have obtained similar results with no *S. aureus* internalization observed upon cytochalasin D treatment of S2 cells, as well as no engulfment of *E. coli* by S2 cells when the assay was carried out at 4ºC. In E and F, wild-type adult flies where injected with pHrodo *E. coli* into their thorax either alone (E) or following pre-injection with 0.9 μm latex beads (F). The lack of fluorescence of the abdomen of the pre-injected male with excess latex beads reflects the lack of engulfment of pHrodo *E. coli* following latex beads pre-injection which saturates the phagocytic abilites of plasmatocytes, thus demonstrating that pHrodo *E. coli* engulfment is via a phagocytic process similar to that of latex beads by plasmatocytes. Similar results were obtained with pHrodo *S. aureus*.

Figure S8: Schematic model implicating UTA, Rya-r44F and the SOCE machinery during DRPR-mediated phagocytosis of apoptotic cells.

Cuttell_Supp Fig.1

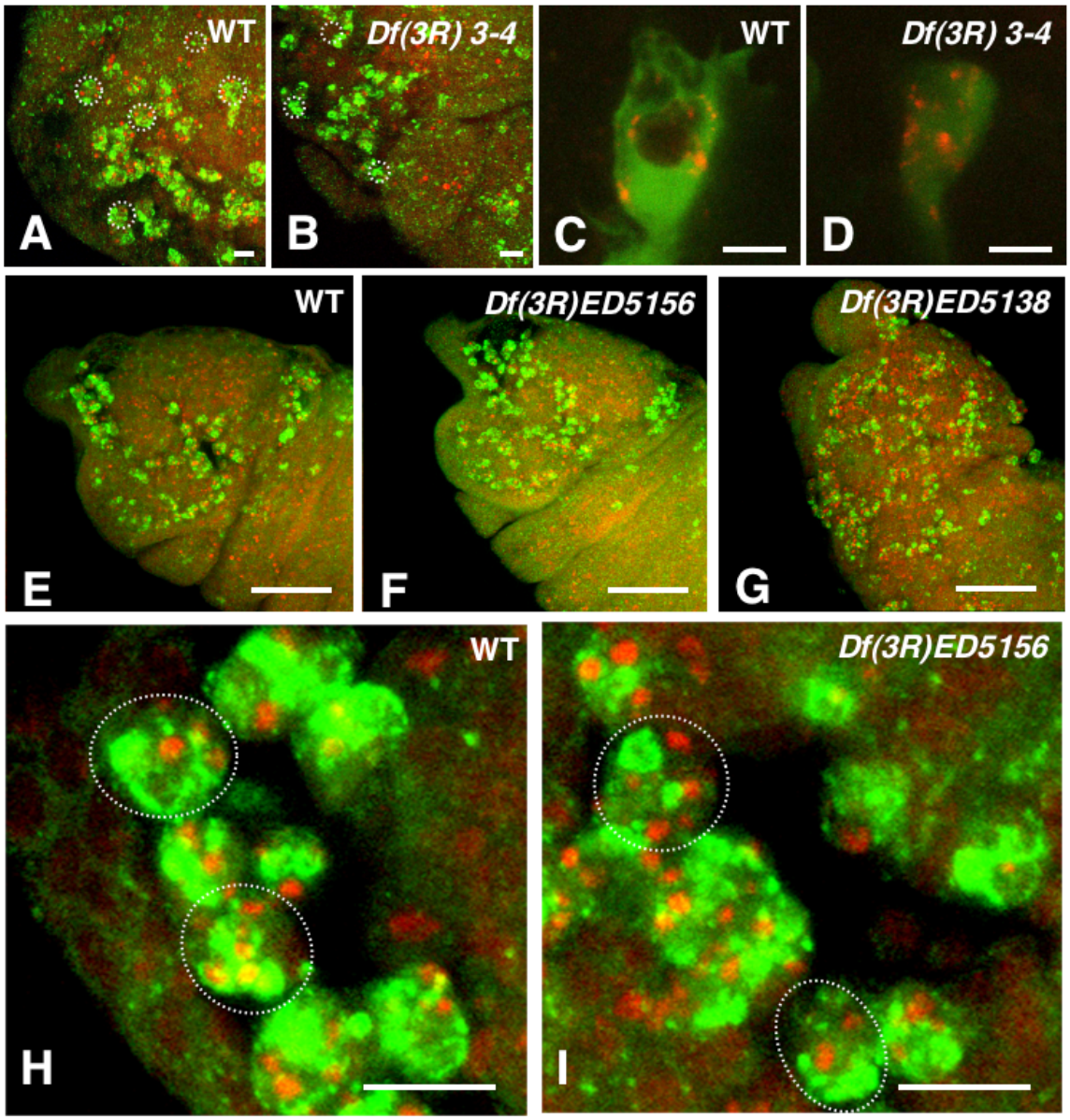

Cuttell_Supp Fig.2

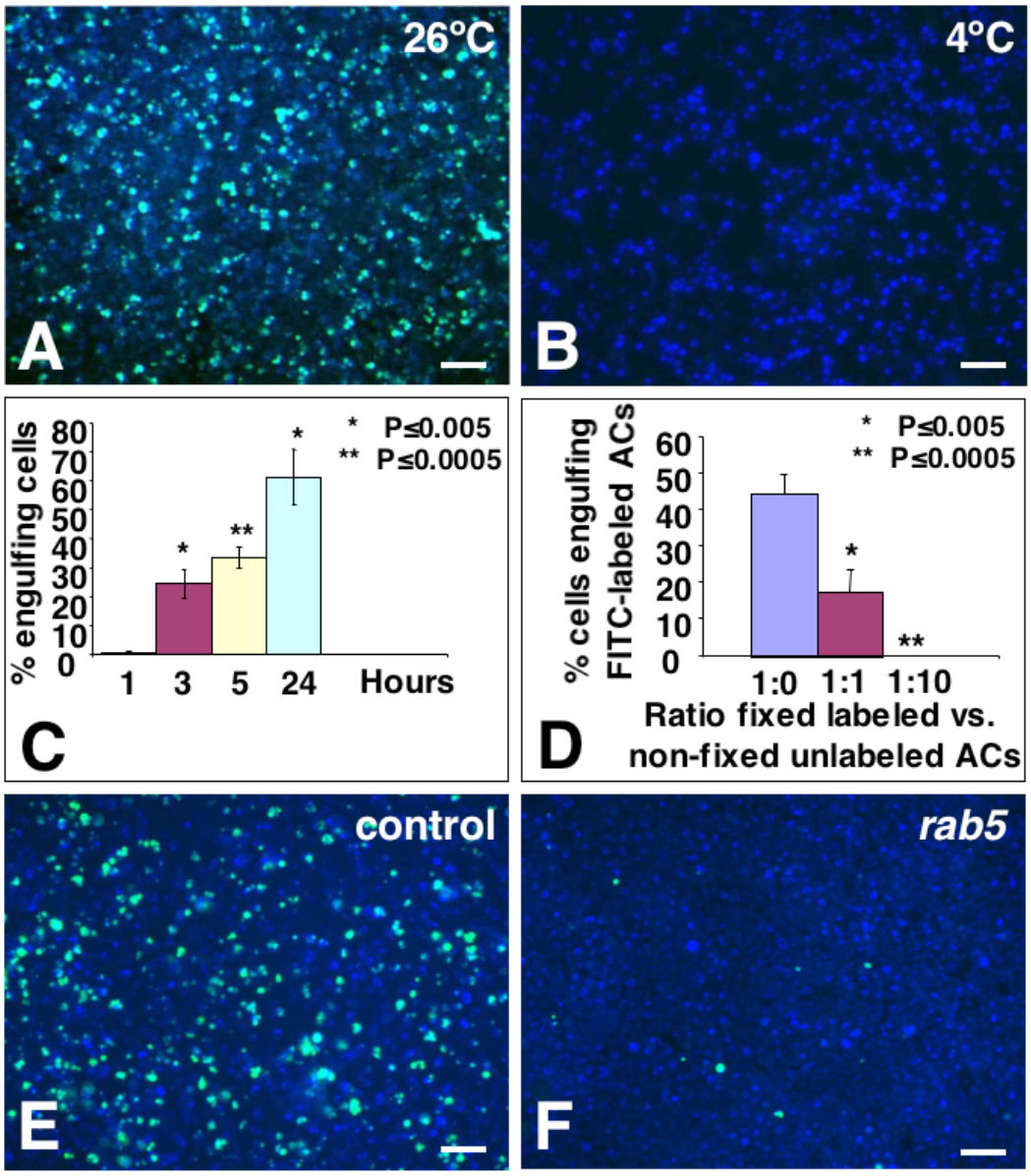

Cuttell_Supp Fig.3

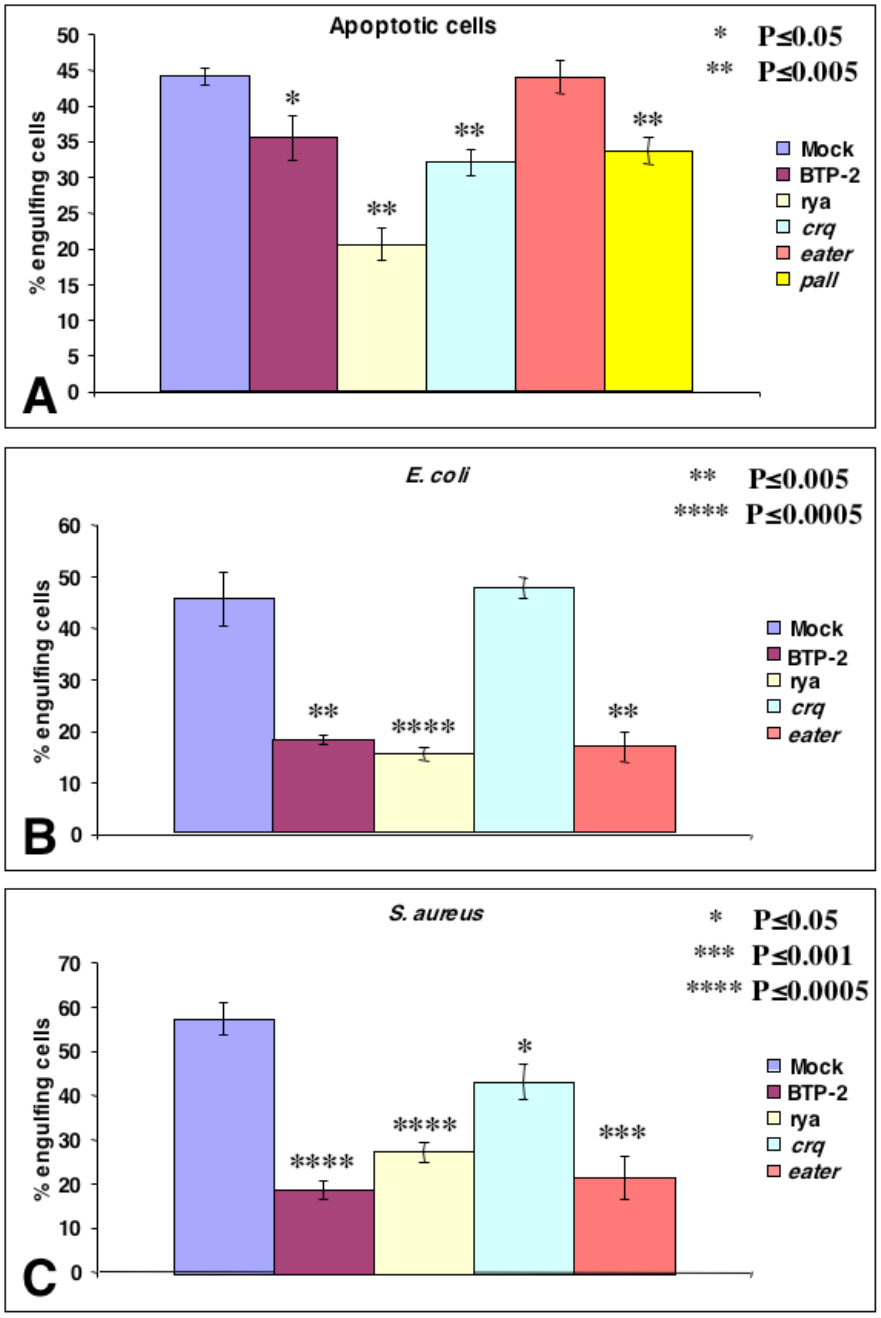

Cuttell_Supp Fig.4

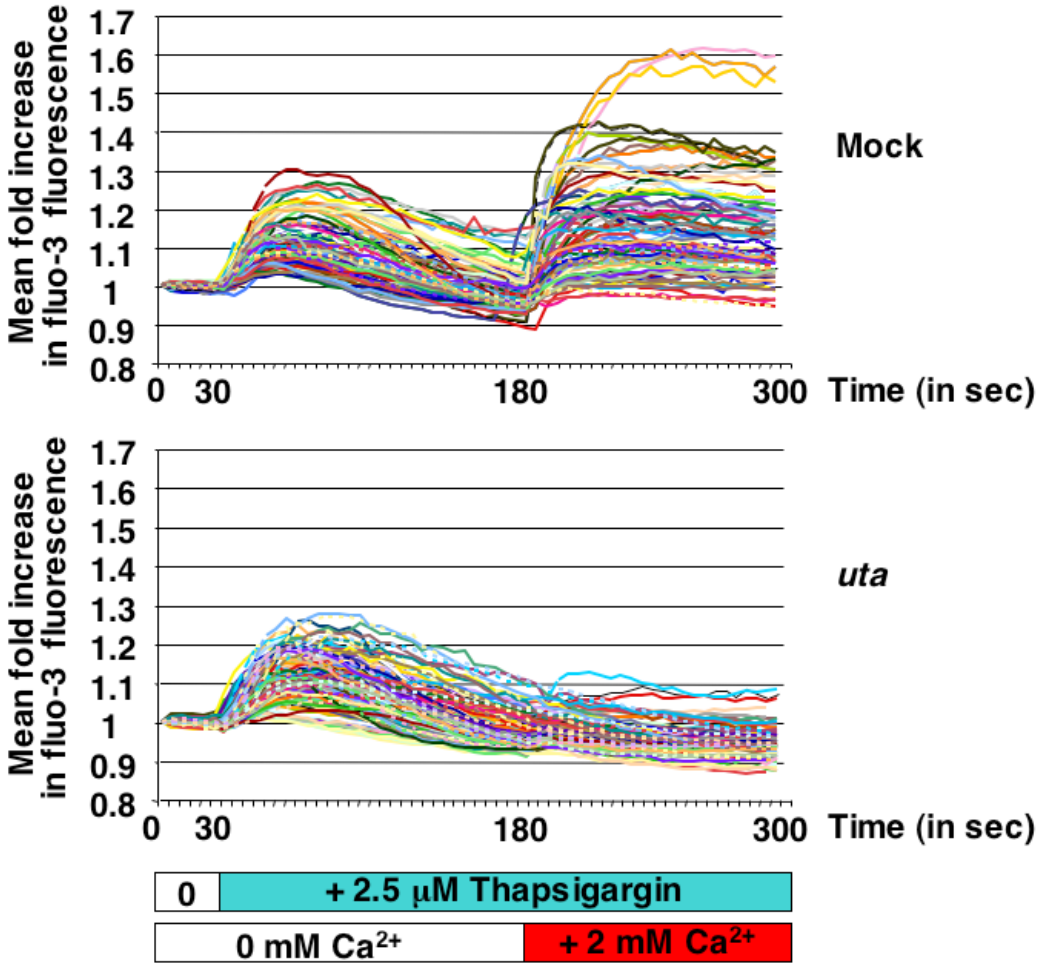

Cuttell_Supp Fig.5

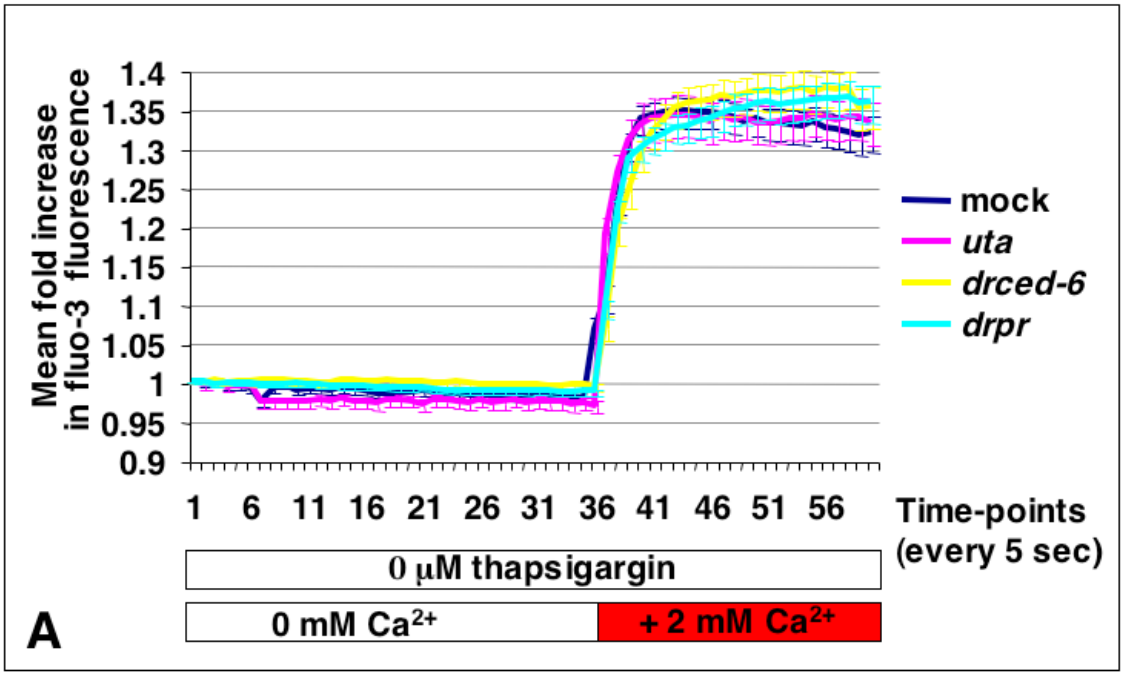

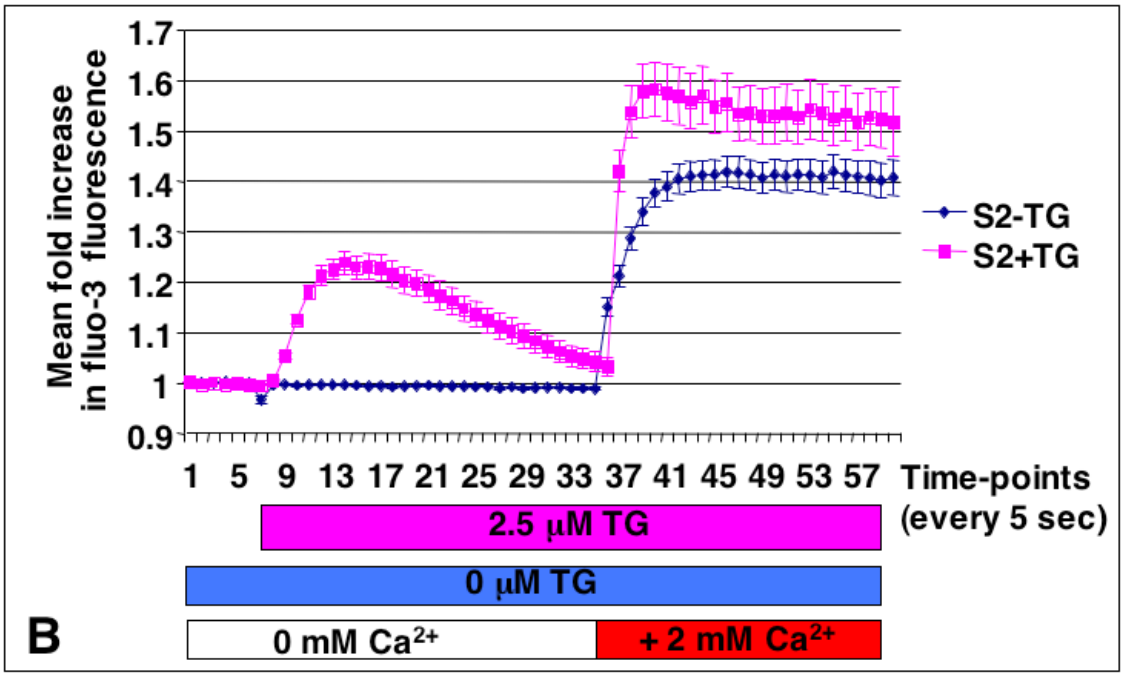

Cuttell_Supp Fig.6

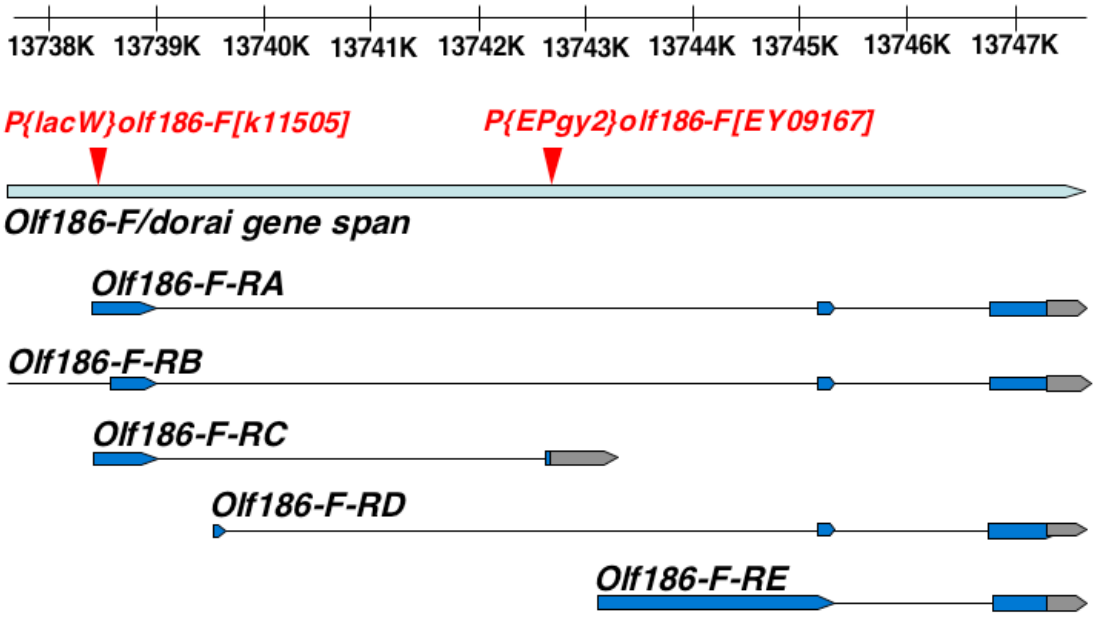

Cuttell_Supp Fig.7

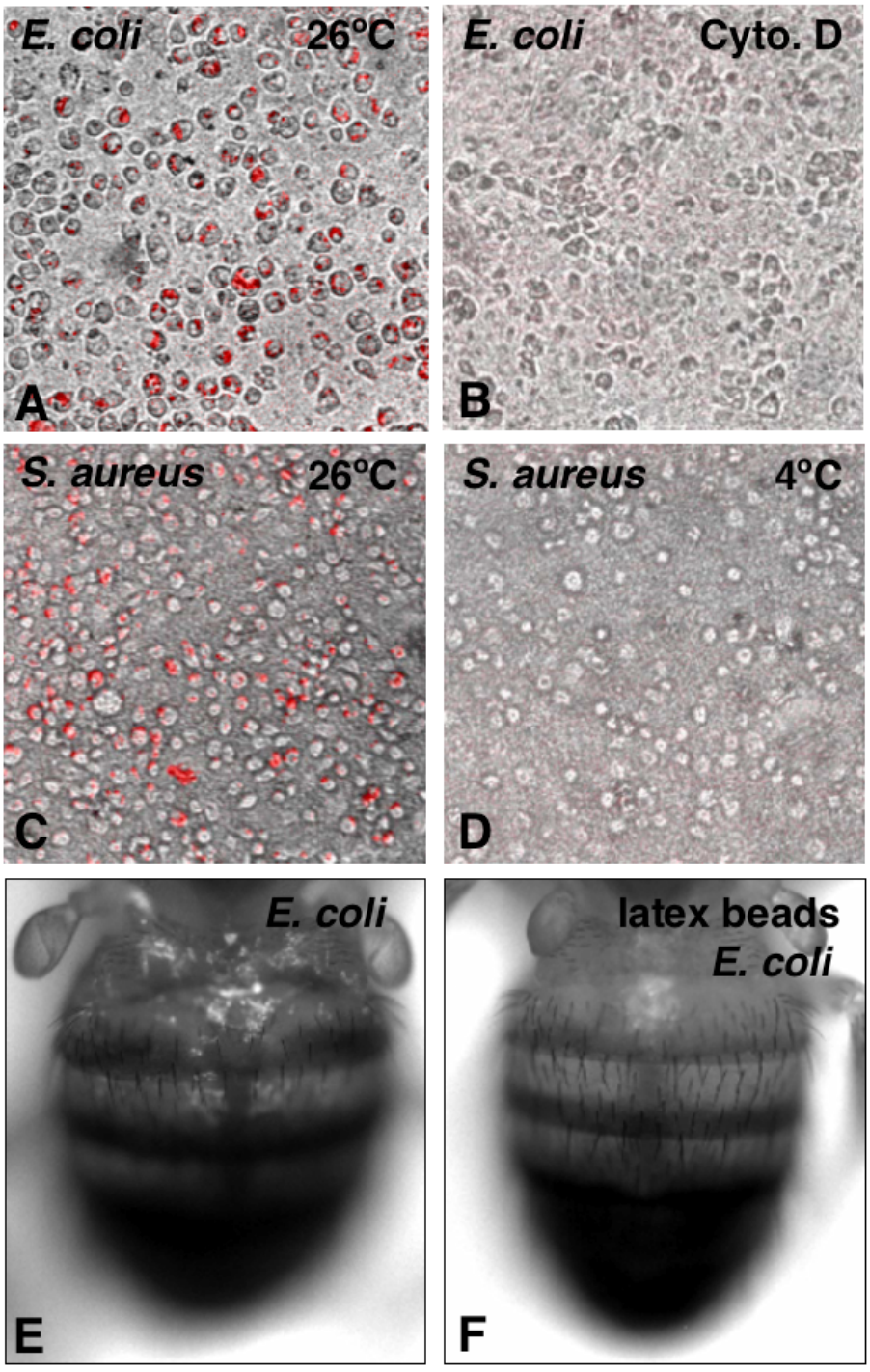

Cuttell_Supp Fig.8

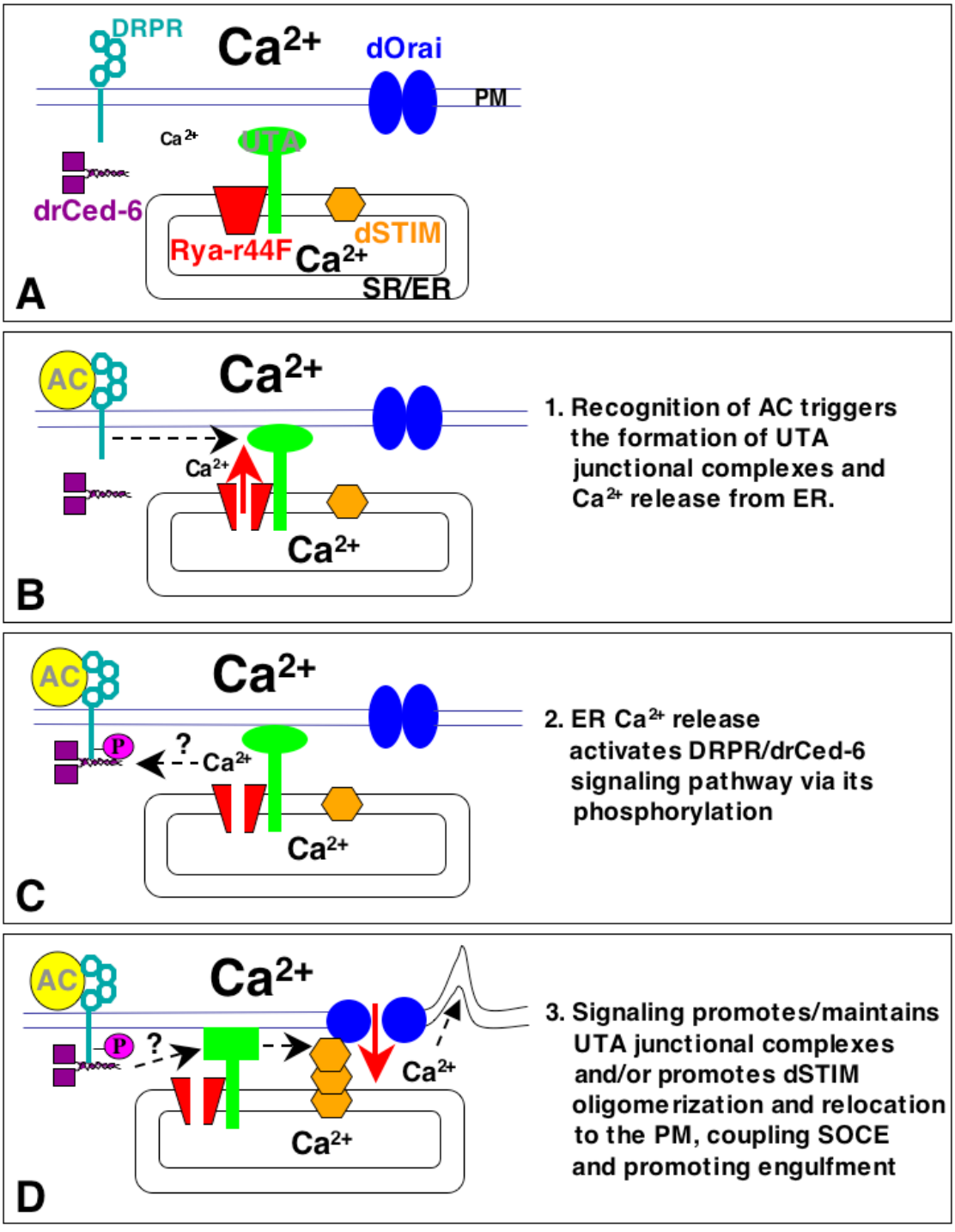

Table S1: Relative qPCR quantification of mRNA level of expression in RNAi-treated S2 cells.

Designation of cell samples	QPCR comparison	Fold difference Relative to Mock S2 cells	Standard deviation
Mock S2	rab5/RpL32	1.000	0.04
Mock S2	uta/RpL32	1.000	0.02
Mock S2	dstim//RpL32	1.000	0.05
Mock S2	dorai/RpL32	1.000	0.03
Mock S2	drced-6/RpL32	1.000	0.03
Mock S2	drpr/RpL32	1.000	0.12
Mock S2	crq/RpL32	1.000	0.06
Mock S2	eater/RpL32	1.000	0.16
Mock S2	pall/RpL32	1.000	0.008
rab5 RNAi	rab5/RpL32	0.295	0.025
uta RNAi	uta/RpL32	0.391	0.051
dstim RNAi	dstim//RpL32	0.217	0.017
dorai RNAi	dorai/RpL32	0.568	0.008
drced-6 RNAi	drced-6/RpL32	0.593	0.023
drpr RNAi	drpr/RpL32	0.509	0.019
crq RNAi	crq/RpL32	0.211	0.015
eater RNAi	eater/RpL32	0.159	0.009
pall RNAi	pall/RpL32	0.228	0.012